ences its hydrodynamic behavior which would be seen in intrinsic viscosity measurements.

The growth of starburst molecules in the present study is using the algorithm of kinetic self-avoiding walk.[15] It is of interest to know whether such an algorithm leads to a faithful description of equilibrium structures of starburst molecules studied experimentally.[7,8] Since it has been shown that a kinetic self-avoiding walk for a linear flexible chain lies in the same universality class[16,17] as the conventional self-avoiding walk in equilibrium, we expect that the conclusions drawn in our study are applicable to the starburst molecules at equilibrium also.

Finally, in an effort to establish the equilivalence between the kinetically grown starburst molecules and equilibrium structures, preliminary development of an algorithm that relaxes the kinetically grown starburst molecules was undertaken. However, initial results indicate that excessive computational time is required to relax these structures due to the large number of particles present. This precludes future work in this area at this time.

Acknowledgment. This work is supported by NSF Grant DMR-8420962. We are grateful to A. D. Meltzer, Prof. D. A. Tirrell, and Prof. D. A. Hoagland for several conversations regarding the problem addressed here.

References and Notes

(1) Zimm, B. H.; Stockmayer, W. H. *J. Chem. Phys.* **1949,** *17,* 1301.
(2) Stauffer, D. *Introduction to Percolation Theory*; Taylor and Francis: London, 1985.
(3) Stauffer, D.; Coniglio, A.; Adam, M. *Adv. Polym. Sci.* **1982,** *44,* 103.
(4) Lubensky, T. C.; Isaacson, J. *Phys. Rev.* **1979,** *A20,* 2130.
(5) Muthukumar, M. *J. Chem. Phys.* **1985,** *83,* 3161.
(6) Daoud, M.; Cotton, J. P. *J. Phys. (Les Ulis, Fr.)* **1982,** *43,* 531.
(7) Tomalia, D. A., et al. *Macromolecules* **1986,** *19,* 2466.
(8) Tomalia, D. A.; Berry, V.; Hall, M.; Hedstrand, D. M. *Macromolecules* **1987,** *20,* 1167.
(9) Maciejewski, M. *J. Macromol. Sci., Chem.* **1982,** *A17* (4), 689.
(10) Edwards, S. F. *Proc. Phys. Soc., London* **1965,** *93,* 605.
(11) de Gennes, P.-G.; Hervet, H. *J. Phys., Lett.* **1983,** *44,* L351.
(12) Naylor, A. M.; Goddard, W. A. *Polym. Prepr. (Am. Chem. Soc., Div. Polym. Chem.)* **1988,** *29* (1), 215.
(13) de Gennes, P.-G. *Scaling Concepts in Polymer Physics*; Cornell University: Ithaca, 1979.
(14) Meltzer, A. D.; Tirrell, D. A. Unpublished results.
(15) Majid, I.; Jan, N.; Coniglio, A.; Stanley, H. E. *Phys. Rev. Lett.* **1984,** *52* (15), 1257.
(16) Peliti, L. *J. Phys., Lett.* **1984,** *45,* L925.
(17) Kremer, K.; Lyklema, J. W. *Phys. Rev. Lett.* **1985,** *55* (19), 2091.

Weak Polyelectrolytes between Two Surfaces: Adsorption and Stabilization

Marcel R. Böhmer,* Olaf A. Evers, and Jan M. H. M. Scheutjens

Laboratory for Physical and Colloid Chemistry, Wageningen Agricultural University, Dreijenplein 6, 6703 HB Wageningen, The Netherlands. *Received June 26, 1989; Revised Manuscript Received October 18, 1989*

ABSTRACT: A theory has been developed for adsorption from solution of weak flexible polyelectrolytes in a gap between two surfaces. The theory is an extension of the self-consistent-field theory of Scheutjens and Fleer for adsorption of uncharged homopolymers. The finite volume of solvent molecules, polyelectrolyte segments, and ions is taken into account using a multi-Stern-layer model. The dielectric constant and the degree of dissociation of polyelectrolyte segments are allowed to vary with position between the surfaces. Results for the potential decay in the electrical double layer are shown. The effect of salt concentration and pH on the adsorption of polyelectrolyte is also studied. With increasing salt concentration more polyelectrolyte chains adsorb and the adsorbed layer becomes more extended. A maximum in the amount of adsorbed polyelectrolyte is found as a function of the counterion concentration. For a polyacid this maximum is at a pH which is 1–1.5 units below pK. Like for uncharged polymers, the interaction between the two surfaces is mainly determined by the adsorbed amount. A low adsorbed amount leads to a deep minimum in the free energy of interaction, due to bridging, at a small separation. A high adsorbed amount leads to a shallow minimum at large surface separation. At smaller separation strong repulsion dominates, due to steric hindrance. If the polyelectrolyte is completely charged, electrostatic repulsion dominates the interaction curve at large separation. As the adsorption depends strongly on salt concentration and pH, the interaction between two surfaces in the presence of an adsorbing polyelectrolyte can in principle be controlled. If the polyelectrolyte does not adsorb, a depletion layer near the surface develops, which becomes thinner with decreasing salt concentration. At small surface separation, when polyelectrolyte has been depleted from between the surfaces, a Donnan equilibrium is established. This results in a stronger attraction than in a situation where electrostatic charges are absent.

Introduction

A few years ago, a theory for the adsorption of linear flexible polyelectrolytes was presented by Van der Schee and Lyklema.[1] These authors showed that electrostatic interactions can be incorporated in lattice-based models for polymer adsorption, such as Roe's model[2] and the self-consistent-field (SCF) theory of Scheutjens and Fleer.[3,4] In these theories the shape of the concentration profile near a surface is not predetermined but is

* To whom all correspondence should be addressed.

0024-9297/90/2223-2288$02.50/0

found by minimizing the free energy. In this way, electrostatic contributions to the free energy directly affect the concentration profile. Van der Schee and Lyklema showed that the strong repulsion between the segments of a polyion leads to very thin adsorbed layers. If this repulsion is screened, e.g. by adding salt, the adsorbed amount increases and the adsorbed layer becomes thicker. The theory of Van der Schee and Lyklema has been extended to weak polyelectrolytes by Evers et al.[5] In this model the degree of dissociation of polyelectrolyte is allowed to vary with the distance from the surface. When H^+ is considered as the counterion of a polyacid, a maximum is found in the adsorbed amount as a function of pH at 1–1.5 units below pK. Both models treat salt ions and hydrogen ions as point charges, whereas the polyelectrolyte segments and the solvent molecules are assigned the same size as a lattice site. The charge of polyelectrolyte segments is located on planes in the centers of the lattice layers. On both sides of each plane an electric double layer is present.

Scheutjens and Fleer extended their theory to polymer adsorption between two flat surfaces. The free energy of interaction between two surfaces in a polymer solution has been calculated.[6,7] If the polymer is allowed to leave the gap between the two surfaces as they approach (full equilibrium), Scheutjens and Fleer find attraction due to bridging. If the polymer is not allowed to escape from the gap (restricted equilibrium), repulsion at small surface separation is found and a minimum in the interaction curve appears. With decreasing amount of polymer, this minimum shifts to smaller surface separation and becomes deeper. Lyklema and Fleer,[8] studying the structure of the adsorbed layer of a strong polyelectrolyte as obtained by the theory of Van der Schee and Lyklema,[1] argued that electrostatic repulsion is dominating the interaction curve at large surface separation. Bridges will not be formed until the surface separation is very small because the adsorbed layers are thin.

In the present paper the SCF theory is extended in such a way that all ions have a volume equal to that of a lattice site. Thus a better description of the adsorbed layer is obtained, and the potential profile turns out to be quite simple. Although we take the SCF theory as the starting point, so that a distinction between segments in trains, loops, and tails can be made, a similar modification can be applied to other lattice models, such as the Roe theory.[2]

It should be noted that the present theory deals with the many-chain problem. This is essential, because most properties of the system depend strongly on the adsorbed amount. Theories for adsorption of a single polyelectrolyte chain have been developed, see, e.g., Muthukumar,[9] but are not applicable when chains interact with each other.

In the Theory section the SCF theory is briefly summarized and the incorporation of electrostatic charges is carried out. The evaluation of the potential profile is explained, and an equation for the free energy of the system is given. In the Results and Discussion section the effect of salt concentration and pH on the adsorption of weak polyelectrolyte is studied. Interaction curves are given as a function of polyelectrolyte charge and adsorbed amount. Some attention is paid to depletion flocculation by fully charged polyelectrolyte.

Theory

Model. The SCF theory is based on a lattice model. The space between two flat surfaces is divided into M parallel lattice layers, numbered $z = 1, 2, ..., M$. The surfaces, adjacent to layers 1 and M, are denoted by layer numbers 0 and $M + 1$, respectively. Each layer contains L lattice sites. A lattice site has Z neighboring sites, of which a fraction λ_0 is found in the same layer and a fraction λ_1 in each of the adjacent layers. In a hexagonal lattice, $\lambda_0 = 6/12$ and $\lambda_1 = 3/12$. A molecule of type i has a volume fraction $\phi_i(z)$ in layer z and ϕ_i^b in the bulk solution. Only inhomogeneities perpendicular to the surfaces are considered and fluctuations within the lattice layers are neglected. A chain molecule consists of r segments, numbered $s = 1, 2, ..., r$, and fills r lattice sites. Solvent (water) molecules and ions are assumed to have the size of one site ($r = 1$). The surfaces are assumed to be smooth and the volume fraction of solid $\phi_S(z)$ is unity in layers 0 and $M + 1$ and zero in between these layers.

Most or all molecules are in full equilibrium with a large bulk solution; i.e., their chemical potential is constant. These molecules are able to rapidly enter or leave the gap between the surfaces as the distance between the surfaces changes. However, on the time scale of variations in surface separation, some molecules, e.g., adsorbed polymer, may be in local equilibrium but restricted in translation to and from the solution. Consequently, the amount of these molecules between the surfaces is constant and their chemical potential is not fixed. This situation is equivalent with a (Donnan) membrane equilibrium, where some of the molecules or ions (polyelectrolytes) cannot pass the membrane. The chemical potential of the molecules in full equilibrium is determined by the composition in the bulk solution.

Segment Density Distribution. In a mixture near a surface a concentration gradient of each type of molecule is present. A segment of molecule type i in layer z is subjected to a potential field $u_i(z)$. This potential, relative to the bulk solution, is given by:

$$u_i(z) = u'(z) + kT\sum_j \chi_{ij}(\langle\phi_j(z)\rangle - \phi_j^b) + v_i\alpha_i(z)e\Psi(z) \quad (1)$$

The term $u'(z)$ represents the local hard-core interaction, which is the same for every type of segment in layer z. It ensures that the sum of all volume fractions of molecules in layer z equals unity. The second term on the right-hand side represents the contact interactions, where χ_{ij} is the Flory–Huggins parameter for the interaction between a segment of type i and Z segments of type j. The sum over j includes the solid in layer 0 and $M + 1$; these terms represent the adsorption energy contributions. The last term on the right-hand side accounts for electrostatic interactions, which are proportional to the valency v_i, of a segment of type i, its degree of dissociation $\alpha_i(z)$ in layer z, and the electrostatic potential $\Psi(z)$ in layer z. The symbols k, T, and e have their usual meaning. The contact fraction, $\langle\phi_i(z)\rangle$, of a site in layer z with segments i is expressed as:

$$\langle\phi_i(z)\rangle = \lambda_1\phi_i(z-1) + \lambda_0\phi_i(z) + \lambda_1\phi_i(z+1) \quad (2)$$

In the bulk solution the contact fraction equals the solution volume fraction for all types of molecules, and all potentials are zero.

The statistical weight of a segment of type i in layer z, with respect to the bulk solution, is given by the segment weighting factor, $G_i(z)$:

$$G_i(z) = \exp(-u_i(z)/kT) \quad (3)$$

If $G_i(z)$ and the solution volume fraction are known, the volume fraction of free monomers of type i follows directly from:

$$\phi_i(z) = \phi_i^b G_i(z) \quad (4)$$

If a molecule contains more than one segment, we should take into account that these segments are interconnected. Segment s of a chain can only be in layer z if segment $s - 1$ is in one of the layers $z - 1$, z, or $z + 1$. We use the end-segment distribution function, $G_i(z,s|1)$, which expresses the average weight of walks along the chain, starting from segment 1, which may be located anywhere in the lattice and ending in layer z after $s - 1$ steps. The end-segment distribution function of a chain of s segments can be expressed in that of a chain of $s - 1$ segments and satisfies a recurrence relation, starting at $G_i(z,1|1) = G_i(z)$:

$$G_i(z,s|1) = G_i(z)[\lambda_1 G_i(z-1,s-1|1) + \lambda_0 G_i(z,s-1|1) + \lambda_1 G_i(z+1,s-1|1)] \quad (5)$$

In the same way we obtain $G_i(z,s|r)$, the end-segment distribution function for chains starting from segment r and ending at segment s. The chain weighting factor, $G_i(r|1)$, of molecules i gives the relative weight for segment r (and hence the chain) to be in the lattice layers between the surfaces:

$$G_i(r|1) = \sum_{z=1}^{M} G_i(z,r|1) \quad (6)$$

This factor will be used as a normalization factor. To obtain the volume fraction, $\phi_i(z,s)$ of segment s in a chain of r segments, the product of two end-segment distribution functions is needed: that of a chain starting at segment 1 and ending at segment s in layer z and that of a chain starting at segment r and also ending at segment s in layer z. This product must be divided by the segment weighting factor of segment s to avoid double counting of this segment. Hence, the volume fraction of segment s in layer z is given by:

$$\phi_i(z,s) = C_i G_i(z,s|1)\, G_i(z,s|r)/G_i(z) \quad (7)$$

where C_i is a normalization constant. Obviously, the total volume fraction, $\phi_i(z)$, of molecules i in layer z can be obtained by summing over s:

$$\phi_i(z) = \sum_{s=1}^{r} \phi_i(z,s) \quad (8)$$

The total amount of molecules i between the two surfaces, expressed in equivalent monolayers, is defined as:

$$\theta_i = \sum_{z=1}^{M} \phi_i(z) \quad (9)$$

If the amount of molecules i between the surfaces is known, the normalization constant C_i can be obtained by normalizing the end-segment distribution function, using eq 6. The total amount of end segments is θ_i/r_i. Thus C_i becomes:

$$C_i = \theta_i/[r_i G_i(r|1)] \quad (10a)$$

Alternatively, C_i can be found from the solution volume fraction. In the bulk solution all G_i's are unity, so that eqs 7 and 8 lead to $\phi_i^b = C_i r_i$ or

$$C_i = \phi_i^b/r_i \quad (10b)$$

From the equations above, the distribution of polymer segments and all other molecules, including small ions, can be calculated from the weighting factors. These distributions determine the spatial arrangement of charges in the system and, consequently, the electrostatic potential profile and should be consistent with eqs 1 and 3. In the next section we describe how the electrostatic potential profile is obtained from the charge distribution, and in Appendix I a numerical procedure is given, which enables the calculation of a self-consistent solution from the full set of equations.

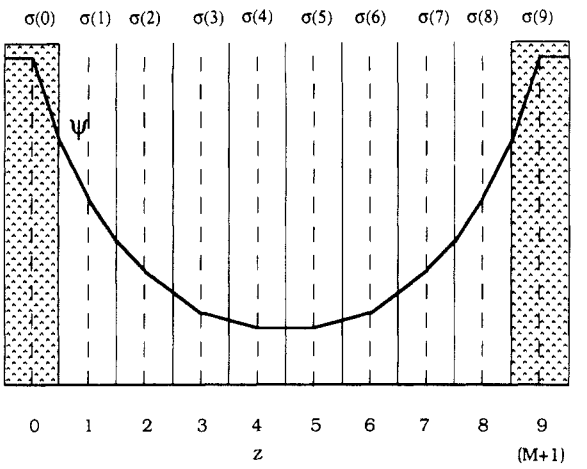

Figure 1. Schematic representation of the lattice and of the electrostatic potential profile. Layers $z = 0$ and $z = 9$ represent the solid surfaces. The electrostatic charges are located on planes in the middle of the lattice layers. The electrostatic potential shows discontinuities at the charged planes due to a change in the electric displacement and between each two lattice layers due to a change in the dielectric constant.

From the density profiles and the weighting factors a very detailed picture of the conformations of the molecules between the plates can be obtained. The adsorbed amount, θ_i^a, is obtained by subtracting from θ_i all chains i that do not touch the surfaces:

$$\theta_i^a = \sum_{z=1}^{M} (\phi_i(z) - \phi_i^f(z)) \quad (11)$$

Free chains do not have segments in layers 1 and M. The volume fraction profile, $\phi_i^f(z)$, of the free chains is found by setting $G_i(1)$ and $G_i(M)$ in eq 5 equal to zero and replacing the end-segment distribution functions in eq 7 by the ones obtained in this way. The calculation of train, loop, tail, and bridge densities and lengths is straightforward.[4,6]

Electrostatic Potentials. The first step in deriving the electrostatic potential profile is the calculation of the charge density in each lattice layer. We assume that the charges are located on the plane in the center of the lattice layer, schematically shown in Figure 1. Outside these planes no electrostatic charge is assumed to be present. We will refer to this model as a multi-Stern-layer model. The plane charge density in layer z is $\sigma(z)$. This quantity is the sum of the contributions of each molecule. If the cross-sectional area per lattice site is a_s:

$$\sigma(z) = \sum_i v_i e \alpha_i(z) \phi_i(z)/a_s \quad (12)$$

The surface charges are located at $z = 0$ and $z = M + 1$ and occur in eq 12 as the term $i = S$, where S is the solid. For weak polyacids the dissociation of a segment is determined by the local volume fractions of H_3O^+ and H_2O. The degree of dissociation $\alpha_i(z)$ in layer z is then given by

$$\alpha_i(z) = \frac{K_i \langle \phi_{H_2O}(z) \rangle}{\langle \phi_{H_3O^+}(z) \rangle + K_i \langle \phi_{H_2O}(z) \rangle} \quad (13)$$

where K_i is the dissociation constant of the polyelectrolyte segments, expressed as a dimensionless parameter.

In practice the dissociation constant K_d is used, which is related to K_i by $K_i = K_d/c_i$, where c_i is the molarity of pure segments i. Because the volume fraction of H_3O^+ and H_2O is not necessarily the same in each layer, variations in the degree of dissociation are automatically accounted for. It is assumed that the association of a charged polyelectrolyte segment with a proton changes neither its size nor its χ parameters.

Since no space charge is present between the charged planes, the electric displacement between two neighboring planes is constant and the electric displacement $D(z)$ is given by:

$$D(z) = \int_{z'=0}^{z} d\sigma(z') = \sum_{z'=0}^{z} \sigma(z') \tag{14}$$

Because of electroneutrality and absence of external fields, the electric displacement is zero outside the system boundaries. From the electric displacement and dielectric constant the electric field strength can be calculated. We assume that the dielectric permittivity, $\epsilon(z)$, in layer z is composed of a linear combination of the dielectric permittivities, ϵ_i, of the molecules:

$$\epsilon(z) = \sum_i \epsilon_i \phi_i(z) \tag{15}$$

The electric field strength, $E(z)$, is

$$E(z) = D(z)/\epsilon(z) \tag{16}$$

and may change discontinuously at each charged plane (due to a change in D) and at each boundary between two lattice layers (due to a change in ϵ). Between these discontinuities in the field strength, the electrostatic potential varies linearly with z. This is analogous to the potential in a charged condenser or in the Stern layer.

Generally, two extremes for charged surfaces are distinguished: either constant surface potential or constant surface charge. Actually, in most systems both the surface potential and the surface charge adapt themselves to local conditions. Although in the present paper we will focus on the case of a constant surface charge and pay some attention to surfaces with a constant potential, our model is applicable to the more general case as well. The simplest way to simulate this is to set the surface charge equal to zero and give the charge-determining ions a strong affinity for the surface, i.e., a negative χ_{iS}, so that a "surface charge" builds up in layers 1 and M.

A constant surface potential is easiest to implement. The total system, i.e., the surfaces and the mixture in between them, is neutral. If the surface potential is given, the surface charge is obtained from the electroneutrality condition: the sum of the surface charges compensates the excess charge in the mixture.

If the surface charge is constant (or zero), the electroneutrality condition requires that the excess charge in the mixture is fixed. The electrostatic potential is undetermined when the field strength in the solid is nonzero. This complicates the numerical calculation of the self-consistent segment density profiles, because the electroneutrality condition should be obeyed at each iteration. In Appendix I, we show how at each iteration the neutrality condition can be obeyed and a reference (Donnan) potential with respect to the bulk solution is calculated.

When the electrostatic potential is known on one plane, the potential on all other planes is easily calculated. In previous models[1,5] the Poisson–Boltzmann equation had to be solved numerically. In the present theory the potential profile is simply obtained by a summation. For instance, if $\Psi(0)$, the potential in the middle of layer 0 (see Figure 1), is known, $\Psi(z)$, the potential in the middle of layer z, is calculated from:

$$\Psi(z) = \Psi(0) - \int_{z'=0}^{z} E(z')\, dz' = \Psi(0) - \frac{d}{2}\sum_{z'=0}^{z}\left\{E(z'-1) + E\left(z' - \frac{1}{2}\right)\right\} \tag{17}$$

In contrast with the SCF theory for uncharged polymers, the distance, d, between two lattice layers and the cross-sectional area, a_s, of a lattice site are explicitly required when electrostatic interactions are involved.

Free Energy of Interaction. The free energy, $A(M)$, of a multi-component system with two surfaces at separation M has been derived by Evers.[10] We extend his equation (51) of Chapter 1 by adding a term that represents the electrostatic energy U_{el}:

$$\frac{A(M)}{LkT} = \sum_i \frac{\theta_i}{r_i} \ln \frac{\theta_i}{G_i(r_i|1)} - \sum_z \sum_i \phi_i(z) \frac{u_i(z)}{kT} + \frac{1}{2}\sum_z \sum_i \sum_j \phi_i(z) \langle \phi_j(z) \rangle \chi_{ij} + \frac{U_{el}}{LkT} \tag{18}$$

The first two terms on the right-hand side of eq 18 have an entropic origin. The third term represents the contribution of the contact interactions, and the fourth term contains the electrostatic contributions. From the free energy at surface separation M, the Gibbs excess free energy, $A^\sigma(M)$, can be obtained by standard thermodynamics:

$$A^\sigma(M) = A(M) - \sum_{i'} \frac{\theta_{i'}}{r_{i'}} \mu_{i'} L \tag{19}$$

The sum extends only over the molecules i' that are in equilibrium with the bulk solution. For these molecules the chemical potential in the mixture between the surfaces is the same as the chemical potential in the bulk solution. The Flory–Huggins equation for the chemical potential μ_i of molecules i in a multi-component system reads:[10]

$$\frac{\mu_i}{kT} = \ln \phi_i^b + 1 - r_i \sum_j \frac{\phi_j^b}{r_j} + r_i \sum_j \phi_j^b \left(\chi_{ij} - \frac{1}{2}\sum_k \chi_{jk} \phi_k^b\right) \tag{20}$$

The free energy of interaction is given by the change in A^σ if the surfaces are brought from infinity to separation M:

$$A^{int}(M) = A^\sigma(M) - A^\sigma(\infty) \tag{21}$$

The electrostatic energy of a multi-layered charged condenser is given by:

$$\frac{U_{el}}{LkT} = \frac{1}{2}\sum_{z=0}^{M+1} \sigma(z)\, \Psi(z) \tag{22}$$

If the surface potential is fixed, energy is gained by placing the excess charge on the surfaces. Verwey and Overbeek[11] showed that this energy gain equals the surface charge times the surface potential, so in the case of a fixed surface potential the electrostatic energy becomes:

$$\frac{U_{el}}{LkT} = -\sigma(0)\, \Psi(0) - \sigma(M+1)\, \Psi(M+1) + \frac{1}{2}\sum_{z=0}^{M+1} \sigma(z)\, \Psi(z) \tag{23}$$

Results and Discussion

In this section we first examine the electrostatic double layer as predicted by our model, in the absence of polyelectrolyte. Subsequently, results are shown for the adsorption of strong and weak polyacid. Finally, the interaction between two surfaces in a polyelectrolyte solution is treated, both for adsorbing and for nonadsorbing polymer.

In the Theory section all concentrations were expressed in volume fractions. In experimental systems, concentrations of small ions are usually given as molarities and we will do the same here. If necessary they can be converted to volume fractions by

$$\phi_i = 10^3 c_i N_A a_s d \tag{24}$$

where c_i is the concentration in moles per cubic decimeter and N_A is Avogadro's number. In a cubic lattice $a_s = d^2$, but we will use a hexagonal lattice throughout this section, for which

$$a_s = (9/8)(2)^{1/2} d^2 \tag{25}$$

The dissociation constant K_d is also expressed in molar concentrations; its relation with K_i as given in eq 13 is $K_d = K_i/(10^3 N_A a_s d)$.

Electrical Double Layers. Solids, such as metal oxides, sulfonated polystyrene latices, etc., in contact with an electrolyte solution can adopt a surface potential of a few hundred millivolts. Such a potential is so high that the concentration of counterions on the surface is limited by the volume of these ions rather than by the surface potential itself. In Figure 2 some examples are given of the decay of the electrostatic potential in the double layer of a surface with a fixed potential of 400 mV. The only molecules present are monovalent ions (salt) and uncharged monomers (solvent). Figure 2a gives the electrostatic potentials as a function of the distance D from the surface for three salt concentrations. The lower the salt concentration is, the lower the surface charge becomes, the more deviation from linearity (on a logarithmic scale) occurs, and the less steep the potential decay is. The curves essentially coincide with analytical calculations using Gouy–Chapman theory in combination with a Stern layer of 0.6 nm. At large D the reciprocal double-layer thickness $\kappa = -\mathrm{d} \ln \Psi/\mathrm{d}D$, as calculated from the potential decay, is $(10.6c_s)^{1/2}$ nm^{-1}, in agreement with the standard expression for the Debye length. In Figure 2b the potential decay for $c_s = 0.1$ M is given for various thicknesses of a lattice layer. Far from the surface, where the volume of the salt ions is not important, all curves are linear and run parallel on the logarithmic scale. Close to the surface the volume of the ions plays a crucial role. If this volume is small, the surface charge can be very high and the initial potential decay is steep. The curve for $d = 0.1$ is nearly indistinguishable from the potential profile as predicted by the Gouy–Chapman theory without Stern layer (i.e., for $d \to 0$). More realistic values for the diameter of a hydrated ion, e.g., $d = 0.6$ nm, lead to a smaller surface charge.

In Figure 2c the potential decay is given in the presence and absence of a strongly adsorbing, uncharged monomer. The potential decay in the first layer is much weaker if adsorbing molecules are present, because less space is left for salt ions. The net effect is that the potential profile shifts slightly to larger distances, in this case about 0.3 nm. This picture does not change when we replace the monomers by uncharged polymer. The shift is mainly due to polymer segments in the first layer where the ion concentration is high. The polymer loops and tails are usually too dilute to affect the potential profile significantly.

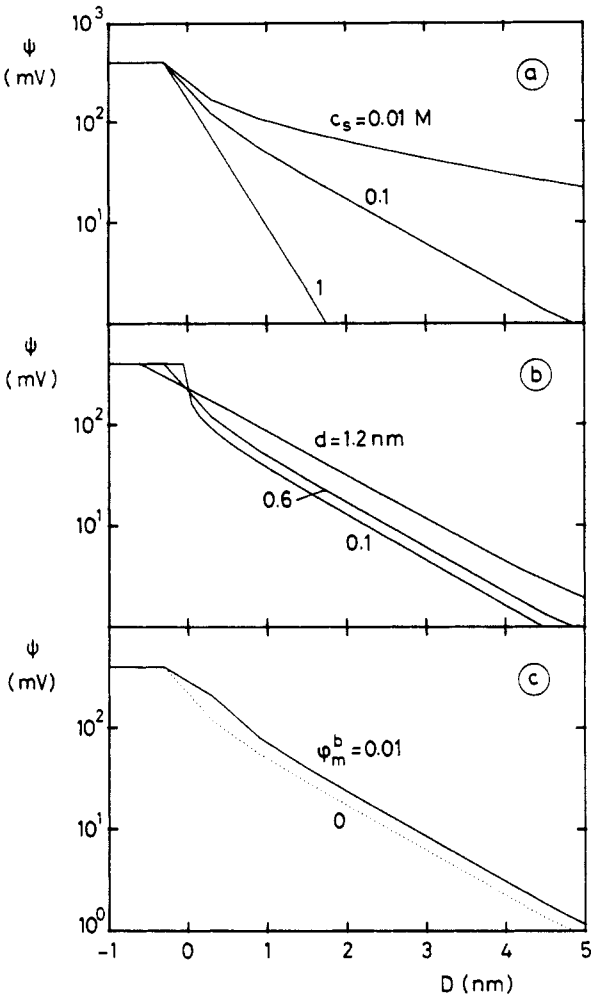

Figure 2. Decay of the electrostatic potential as a function of the distance from the surface in the presence of monovalent ions. The surface potential $\Psi(0)$ is 400 mV. $D = 0$ corresponds to the boundary between solid and liquid. A hexagonal lattice is used ($\lambda_0 = 6/12$). For all molecules $\epsilon = 80\epsilon_0$. All Flory–Huggins interaction parameters are zero. (a) Potential profiles in three different salt concentrations: $c_s = 0.01$, 0.1, and 1 M. The thickness of a lattice layer d is 0.6 nm and the centers of the surface atoms are at $D = -0.3$ nm. (b) Potential profiles at various thicknesses of the lattice layers: $d = 0.1$, 0.6, and 1.2 nm. The centers of the surface atoms are at $D = -0.05$, -0.3, and -0.6 nm, respectively; $c_s = 0.1$ M. (c) Potential profiles in the presence (full curve) and absence (dotted curve) of a strongly adsorbing uncharged monomer m. $c_s = 0.1$ M, $d = 0.6$ nm, $\chi_{mS} = -40$.

Carney and Torrie[12] compared the results of Monte Carlo (MC) simulations with calculations using the Gouy–Chapman theory extended with a Stern layer. They showed that for a 1–1 electrolyte at moderate concentrations ($c_s < 0.1$ M) the agreement between the extended Gouy–Chapman theory and the MC simulations is good when the surface charge is not too high ($\sigma(0) < 50$ mC/m^2). The agreement was found to be reasonable for surface charges up to 300 mC/m^2 and also for higher electrolyte concentrations. These observations in combination with Figure 2 lead to the conclusion that the multi-Stern-layer model is very suitable for the incorporation of electrostatic interactions in lattice theories. Additional advantages of our model, as far as its application on double-layer phenomena is concerned, are that nonelectrostatic interactions, such as specific adsorption of ions and other nearest-neighbor interactions, can be accounted for by the χ parameters. If the surface charge

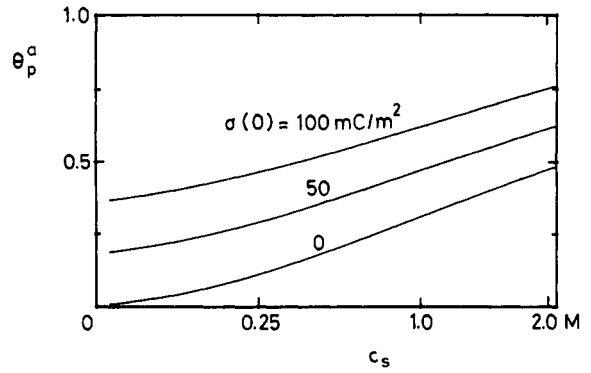

Figure 3. Adsorbed amount, θ_p^a, of a fully dissociated, negatively charged polyelectrolyte as a function of the salt concentration on a square-root scale for three values of a constant surface charge: $\sigma(0)$ = 0, 50, and 100 mC/m^2. The Flory–Huggins interaction parameter, χ_{pS}, between surface and polymer is −4, and for the polymer–solvent and polymer–salt interactions, χ = 0.5. The remaining interaction parameters are zero. The relative dielectric constants of the polyelectrolyte and the surface are 20 and that of the other molecules is 80. The chain length r_p, of the polymer is 500, and the solution volume fraction ϕ_p^b is 10^{-4}. Hexagonal lattice, d = 0.6 nm.

is so high that the volume of ions affects the potential profile over more than one molecular diameter, the multi-Stern-layer model is expected to give a better description than the Gouy–Chapman theory extended with a single Stern layer.

Adsorption of Strong Polyelectrolyte. All calculations in this section have been performed assuming a hexagonal lattice with a layer thickness of 0.6 nm (a_s = 0.573 nm^2). Polyelectrolyte chains considered here are polyanions of 500 segments long having a relative dielectric constant of 20. The χ values for the interaction between polyelectrolyte segments and solvent or salt ions are 0.5. The χ parameters for salt ion–solvent interactions are taken to be zero. The Flory–Huggins parameter, χ_{pS}, for the interaction between a polyelectrolyte segment and the surface is chosen to be −4, representing a net attraction relative to the small molecules, for which χ_{iS} is set to zero. As only a fraction λ_1 of an adsorbed segment is in actual contact with the surface, the net adsorption energy of the polymer (in units of kT per segment, where k is Boltzmann's constant and T the temperature) is $-\lambda_1(\chi_{pS} - \chi_{iS})$ = 1. The effects of varying this adsorption energy will not be shown here; the trends are the same as given in the paper by Evers et al.[5] The volume fraction of polyelectrolyte in the bulk solution is 100 ppm. The relative dielectric constant of all components except the polymer equals 80. The surface charge $\sigma(0)$ = 50 mC/m^2, unless stated otherwise. This corresponds to 0.179 elementary charges per surface site.

In Figure 3 the adsorbed amount, θ_p^a, of a strong polyelectrolyte on one oppositely charged surface, expressed in equivalent monolayers, is given as a function of the square root of the salt concentration (which is proportional to the reciprocal double-layer thickness) for three values of a fixed surface charge: $\sigma(0)$ = 0, 50, and 100 mC/m^2. For all surface charges adsorption increases with salt concentration. Even in salt concentrations around 1 M, addition of more salt still enhances adsorption. This is due to penetration of salt ions between the polyelectrolyte segments and the concomitant reduction of segment–segment repulsion. If penetration of salt ions is impossible, e.g., in the case of a bare and smooth surface, changes in the salt concentrations above 0.1 M hardly affect the properties of the system, e.g., double-layer characteristics and the stability of hydrophobic colloids. Experimentally, an increase in the amount of adsorbed polyelectrolyte as a function of ionic strength has indeed been found up to high salt concentrations.[13-16]

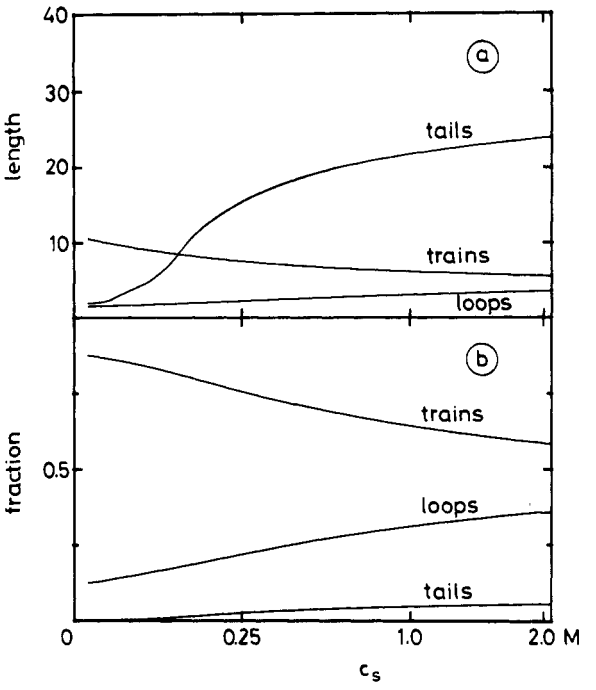

Figure 4. Average length (a) and the fraction (b) of segments in trains, loops, and tails as a function of the square root of the salt concentration for a strong polyelectrolyte adsorbing on a surface with a fixed surface charge of 50 mC/m^2. The other parameters are the same as in Figure 3.

The curves for different surface charges are almost parallel. The adsorption of polyelectrolyte increases linearly with the surface charge, in agreement with the model of Evers et al.[5] If the surface is uncharged, the adsorbed amount is very low and depends strongly on c_s at all salt concentrations. If the surface and polyelectrolyte are oppositely charged, the adsorbed amount at low salt concentrations is nearly independent of c_s and only slightly higher than necessary for neutralization of the surface charge. The surface charge determines the adsorbed amount at low salt concentrations. This is corroborated by measurements of Blaakmeer et al.,[17] who recently found that an increase in the salt concentration from 0.001 to 0.1 M hardly changed the adsorption of polyelectrolyte on a latex with a high surface charge.

The increase in the adsorption with salt concentration is roughly the same for all surface charges studied. To be more precise, we note that the slope is slightly higher at low surface charges. This is due to the weaker repulsion between segments of adsorbed chains, when the total amount of adsorbed polyelectrolyte is smaller.

At low salt concentrations, the polyelectrolyte adsorbs in very flat conformations. Around 90% of the segments of adsorbed chains are in contact with the surface, tails are almost absent and the few loops are short; see Figure 4. In this figure the situation for $\sigma(0)$ = 50 mC/m^2 is plotted. Flat adsorption of polyelectrolyte has been found experimentally, using small-angle neutron scattering, by Cosgrove et al.[16] and, using ESR, by Cafe and Robb.[18] As shown in Figure 4a the average train length is reduced with increasing salt concentration, whereas tails and loops become longer. The same trends show up in Figure 4b: the fraction of segments in trains becomes lower with rising ionic strength, whereas the fraction of segments in loops and tails becomes larger. Although the fraction of segments in trains becomes smaller, the vol-

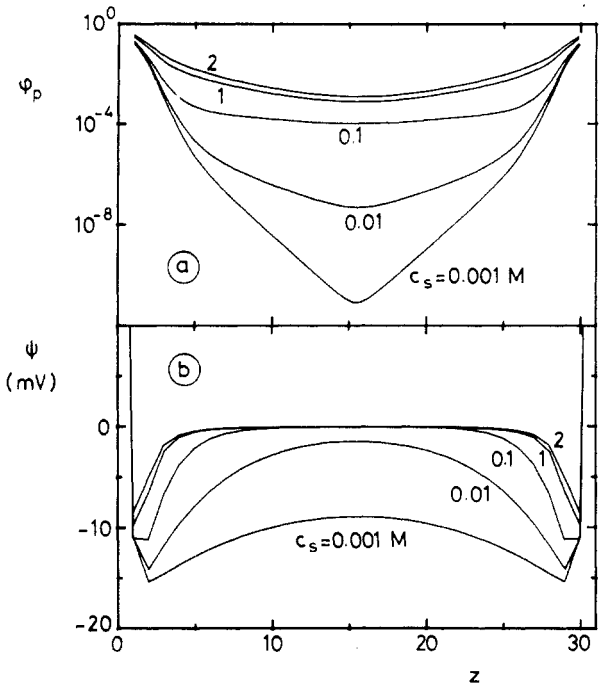

Figure 5. Volume fraction profiles (a) and the corresponding potential profiles (b) of strong polyelectrolyte between two surfaces with a fixed surface charge of 50 mC/m^2 and 30 lattice layers apart, for five salt concentrations. Same parameters as in Figure 3. The surface potential is around 100 mV (not shown).

ume fraction in layer 1 increases because of the higher adsorption.

In Figure 5a the volume fraction profiles of a strong polyelectrolyte between two surfaces, which are 30 lattice layers apart, are given for five salt concentrations. The volume fraction of polyelectrolyte segments decreases very strongly with increasing distance from the surface. In low salt concentrations the decay of the volume fraction of polyelectrolyte is steeper than that in high salt concentrations and the volume fractions in the middle layers reach values far below the solution volume fraction of 100 ppm. At low salt concentrations free polyelectrolyte chains are almost absent between the surfaces. The reason why depletion occurs can be deduced from the potential profiles given in Figure 5b. The surface potential stabilizes around 100 mV at all salt concentrations (not shown). The adsorbed polyelectrolyte causes a charge reversal in the first layer, leading to a negative potential in layers 1 and M. In high salt concentrations the charge reversal is weak and the negative potential is effectively screened. In low ionic strength, a stronger charge reversal occurs and it is more difficult to screen the resulting potential; both effects are due to the fact that salt ions are scarce. This leads to a negative potential everywhere between the surfaces, and the negatively charged free chains are depleted. These results are extensions of the profiles calculated by Van der Schee and Lyklema[1] for polyelectrolyte adsorption on one surface.

Adsorption of Weak Polyelectrolyte. In the following series of calculations each polyelectrolyte segment has been given a dissociation constant K_d, with pK_d = 5. The counterion is H_3O^+. Calculations of polyelectrolyte adsorption on one surface are performed for a salt concentration of 0.1 M and three values of a constant surface charge: 0, 50, and 100 mC/m^2.

The adsorption as a function of pH is given in Figure 6a. At high pH, where the polymer is fully charged, the situation is similar to that in the previous section and,

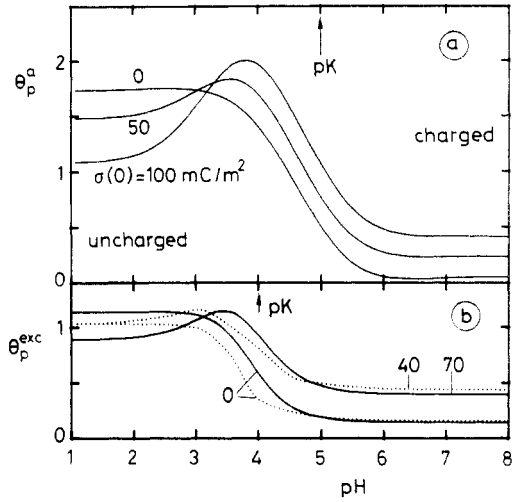

Figure 6. (a) Adsorbed amount of a weak polyacid as a function of pH for three fixed surface charges: 0, 50, and 100 mC/m^2, pK_d = 5, c_s = 0.1 M. Other parameters as in Figure 3. (b) Excess amount of a weak polyacid as a function of pH as calculated by Evers et al.[5] (dotted curves) and according to the present model (full curves). All χ parameters are set to zero except χ_{pS} = −2, and the interaction parameter between polymer segments and the other molecules equals 0.5. The chain length is 500 segments, the dielectric constant of the polyelectrolyte is $3\epsilon_0$, and other dielectric constants are $80\epsilon_0$, pK_d = 4, c_s = 1 M, λ_0 = 0.5. For the results by Evers et al., d = 1 nm, a_s = 1 nm^2, and the surface charges are 40 mC/m^2 (0.25 charges/lattice site) and 0 mC/m^2. For our model: d = 0.6 nm, a_s = 0.573 nm^2, and the surface charges are 70 mC/m^2 (0.25 charges/lattice site) and 0 mC/m^2.

consequently, the adsorbed amount is low. A positive surface charge leads to more adsorption because there is more charge to be neutralized. As the pH decreases, the charge on the polyelectrolyte reduces, so that the segment–segment repulsion becomes less important and the adsorbed amount increases. This has been shown experimentally as well.[17,19,20]

If the surface and the polyacid are oppositely charged and χ_{pS} is small, a maximum occurs in the adsorbed amount around 1–1.5 pH units below pK, which has also been predicted by Evers et al.[5] In the maximum the surface charge density is about the same as the charge density of adsorbed polyelectrolyte. The overall polyelectrolyte charge, and thus the lateral repulsion between the segments, is small. Depending on the surface charge, the degree of dissociation in the first layer adjusts itself such that the surface charge can be neutralized, even if the pH in the bulk solution is 1 or 2 units below the pK. However, if the pH is too low, the charge of the polyelectrolyte will be decreased. The attractive electrostatic interaction between polyelectrolyte and surface vanishes, and hence the adsorbed amount decreases, slightly depending on the adsorption energy. At low pH the polyelectrolyte cannot screen the surface charge so that the electrostatic potential in layer 1 increases and negative salt ions adsorb more strongly. Because of their finite volume, these ions displace polyelectrolyte segments from the surface. This causes a further reduction in the adsorbed amount, especially if the surface charge is high.

In Figure 6b we compare our results (full curves) with results obtained by Evers et al.[5] (dotted curves) in more detail. Evers et al. present the excess adsorbed amount, θ_p^{exc}, for d = 1 nm, a_s = 1 nm^2, and c_s = 1 M. The high salt concentration and big lattice cells uncover immediately a few typical differences between the two theories. We cannot choose such a high value for the cell volume, since we allow only one ion per cell, so that the maxi-

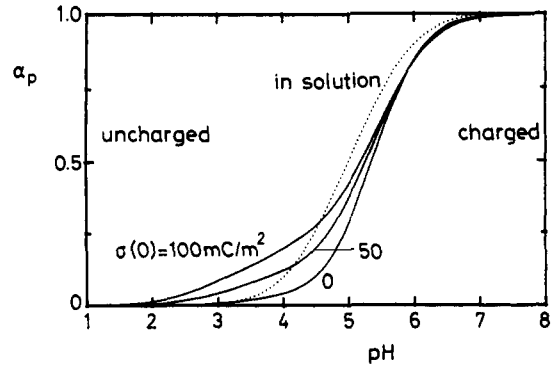

Figure 7. Degree of dissociation as a function of pH of a free segment in bulk solution (dotted curve) and a polyelectrolyte segment on the surface for three different surface charges (full curves). See Figure 6 for the parameters.

mum salt concentration would be about 0.8 M (see eq 24). Therefore, we choose again d = 0.6 and a_s = 0.573 nm^2 for our model. The adsorption in Figure 6b is lower than that in Figure 6a because the adsorption energies are χ_{pS} = −2 and −4, respectively. We first discuss the situation at pH = 1. As for uncharged polymer both d and a_s are not required in the theory; the adsorption at pH = 1 (where the dotted curves coincide) is independent of the segment size. Yet the present model predicts a slightly higher adsorption on uncharged surfaces. This is a well-known effect of using the SF approach instead of Roe's model.[3] In the model of Evers et al. the adsorption of uncharged polymer is independent of the surface charge, because the salt ions are treated as point charges and hence cannot displace the polymer by steric interactions. Thus the volume of ions is responsible for the more pronounced maximum in the full curves.

At pH = 7, the polymer is fully charged; the adsorption at $\sigma(0)$ = 40 mC/m^2 in the Evers model is almost the same as that at $\sigma(0)$ = 70 mC/m^2 in our model. This is to be expected because of the decrease in a_s by a factor of 7/4 and, consequently, the given increase in the surface charge is necessary to compensate the increased polymer charge. Another starting point to explain this correspondence is that the surface charge per site equals 0.25 elementary charges in both models. In other words, for fully charged polymer the adsorption energy per segment (in this case χ_{pS} = −2) and the charge per surface site (0.25) determine the adsorbed amount, leading to essentially the same adsorption in both models.

The full curves are shifted to a slightly higher pH with respect to the dotted curves. This is due to the big volume of salt ions, which, at this high concentration, considerably lowers the volume fraction of free water and thus the degree of dissociation of the polymer (see eq 13).

Experimentally, it is difficult to measure polyelectrolyte adsorption far below the pK. Durand-Piana et al.[21] measured the adsorption of a random copolymer at various percentages of charged segments. In their study a maximum in the adsorption was found at 1% of charged segments. Recently, Blaakmeer et al.[17] measured the adsorption of polyacrylic acid as a function of pH. These authors found a maximum in the adsorption at pK = 2, which is in agreement with our calculated results.

In Figure 7 the degree of dissociation of a free segment in the bulk solution as a function of pH is compared with that of a polyelectrolyte segment in the first layer. At conditions are the same as in Figure 6. Even though a mean-field approximation is used, the model predicts that the accumulation of charged segments in

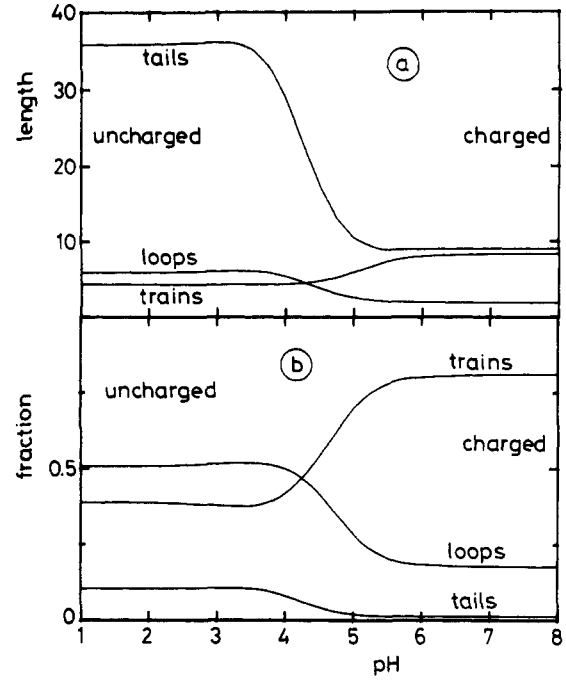

Figure 8. Average length (a) and fraction (b) of segments in trains, loops, and tails as a function of pH. For parameters, see Figure 6; $\sigma(0)$ = 50 mC/m^2.

layer 1 suppresses dissociation significantly when the surface is uncharged. It should be noted that the volume fraction of segments in the first layer is not constant, because the adsorbed amount changes with pH. When the surface charge is positive, the degree of dissociation in the first layer at low pH is higher than in the bulk solution. In order to effectively neutralize the surface charge the polyelectrolyte adjusts its degree of dissociation.

In Figure 8 the average length and fraction of segments in trains, loops, and tails as a function of pH are given for $\sigma(0)$ = 50 mC/m^2. The length and fraction of loops and tails decrease with increasing pH, whereas the fraction and average length of trains increase. The electrostatic repulsion between the segments is reduced by lowering the pH, which leads to the development of loops and tails just as in the case of a rising salt concentration. However, the effect of pH on the adsorbed amount is much more pronounced than the influence of ionic strength. A reduction of the polyelectrolyte charge has a more drastic effect on the adsorbed amount than screening the polyelectrolyte charge by the addition of salt. Therefore, caution should be taken when comparing the adsorption of polyelectrolyte at high ionic strength with the adsorption of uncharged polymers.

Interaction between Two Surfaces in the Presence of Adsorbing Polyelectrolyte. Interaction curves are given for a fixed surface charge of 50 mC/m^2. All other parameters have the same values as in the previous section. The amount of polymer between the surfaces is assumed to be independent of the surface separation (restricted equilibrium). For simplicity, the van der Waals attraction between the surfaces has been omitted, as its contribution is relatively small and depends on the properties of the solids.

In Figure 9a the interaction curves for a weak polyacid are given for three pH values. The free energy is given in units of kT per surface site (a_s = 0.573 nm^2). Obviously, the total free energy of interaction is proportional to the surface area. The amount of polyacid between the surfaces corresponds to the equilibrium adsorption

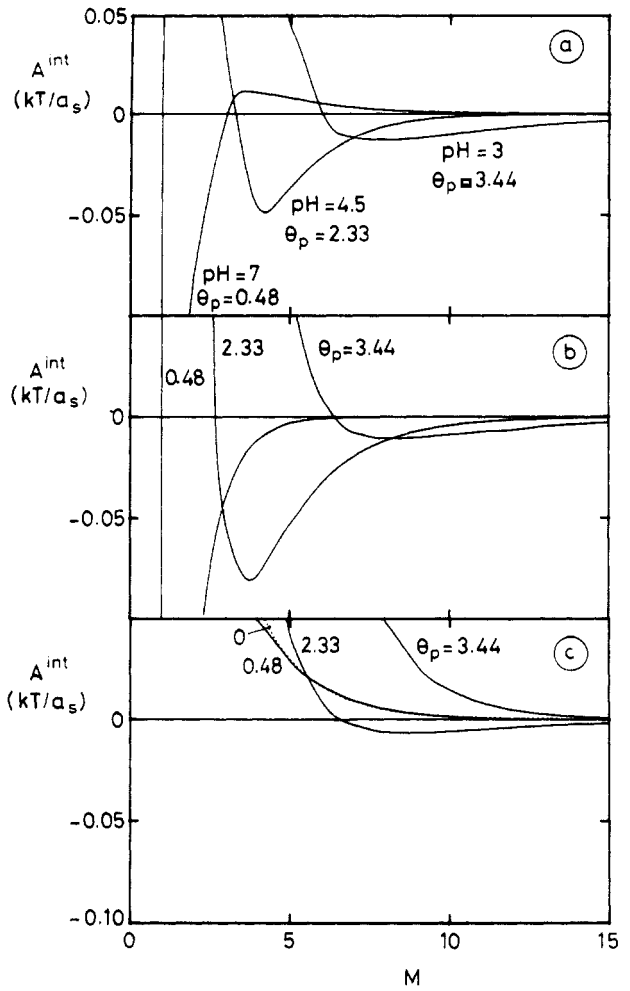

Figure 9. Interaction between two surfaces covered with (a) polyelectrolyte at three pH values or (b,c) an equal amount of uncharged polymer. The surface charge $\sigma(0)$ is 50 mC/m^2 (a,c) or zero (b). For the other parameters, see Figure 6. The amount of polyelectrolyte or polymer between the surfaces is fixed (restricted equilibrium) and equals the equilibrium amount of polyelectrolyte between the surfaces at separation M = 60 in a solution of volume fraction 100 ppm. The amounts between the surfaces are as follows: for pH = 7.0, θ_p = 0.48; for pH = 4.5, θ_p = 2.33; for pH = 3.0, θ_p = 3.44. In (c) the interaction curve in the absence of polymer is also given (dotted curve).

at a solution volume fraction of 100 ppm when the surfaces are 60 lattice layers apart. At pH = 7.0 the polyelectrolyte is almost fully dissociated. Consequently, the amount between the surfaces is small: θ_p = 0.48 equivalent monolayers. As the surfaces are brought closer, the free energy of interaction passes a maximum, i.e., a repulsive barrier is present, as anticipated by Lyklema and Fleer.[8] At a surface separation smaller than three lattice layers, the curve shows a very deep minimum. The thickness of polyacid segments prevents the surfaces from approaching closer than one layer: A^{int} is infinite for M < 1. At pH = 4.5 more polyelectrolyte is present between the surfaces: θ_p = 2.33. At this pH the interaction curve shows a weaker minimum, which is situated at a larger surface separation, and the maximum is absent. Another interaction curve is given for pH = 3.0, where θ_p has increased to 3.44. Again the minimum in A^{int} is weaker and located at a still larger surface separation.

To analyze the data in Figure 9a more quantitatively in terms of contributions from the surface charge, polyelectrolyte charge, and steric effects (bridging, steric repulsion), calculations were performed with the same amounts of uncharged polymer between two uncharged surfaces (Figure 9b) and between charged surfaces (Figure 9c). The shapes of the curves in Figure 9b are similar to those in Figure 9a. At the smallest amount of uncharged polymer, θ_p = 0.48, which corresponds to pH = 7.0 in the case of a weak polyacid, the interaction is always attractive (except for M < 1). This attraction is known to be caused by polymer bridging.[6] If θ_p is 2.33 (the value for weak polyacid at pH = 4.5), the bridging attraction is stronger, but at surface separations smaller than three lattice layers, steric repulsion dominates. Finally at θ_p = 3.44, which corresponds to pH = 3.0 in the case of weak polyacid, both bridging attraction and steric repulsion set in at even larger surface separation. As a result of this, the minimum has further shifted to a larger separation and has become shallow. Interaction curves for uncharged polymers have been discussed in detail elsewhere.[6]

The calculations presented in Figure 9c are for the same uncharged polymer as in Figure 9b, but now the surfaces are charged. The surfaces have been given a fixed charge of 50 mC/m^2, and the amounts of polymer between the surfaces are the same as in parts a and b of Figure 9. For the smallest amount of polymer between the surfaces, θ_p = 0.48, the interaction between the surfaces is repulsive at all surface separations and almost indistinguishable from the interaction in the absence of polymer, as shown in the same figure (θ_p = 0, dotted curve). It can be concluded that this repulsion is purely electrostatic, the more so since this small amount of polymer cannot cause steric repulsion, according to Figure 9b. Also at larger amounts of polymer the electrostatic repulsion has a pronounced effect on the interaction. At θ_p = 2.33 the minimum has become less deep and has shifted to a larger surface separation as compared to the case of uncharged surfaces. At θ_p = 3.44 the minimum has vanished and more repulsion is found than in the absence of electrostatic charges. The decay of the electrostatic potential is hampered by the large amount of polymer and thus causes a stronger electrostatic repulsion at a relatively large surface separation than in the absence of polymer.

If we return to Figure 9a, it becomes clear that the interaction between two surfaces in the presence of adsorbing polyelectrolyte resembles Figure 9b rather than Figure 9c: the interaction is mainly determined by the amount of polymer present. At all pH values the surface charge is effectively neutralized by polyelectrolyte. The surface charge is slightly overcompensated by the adsorption of polyelectrolyte at the χ_{ps} value chosen (see, e.g., Figure 5b). This overcompensation manifests itself in the repulsive part of the interaction curve at pH = 7 and in the depth of the minimum at pH = 4.5 compared to θ_p = 2.33 in Figure 9b.

Direct force measurements by Afshar-Rad et al.[22] on small amounts of poly-L-lysine adsorbed between mica sheets showed an interaction curve similar to the curve in Figure 9a for pH = 7. For several proteins a higher adsorption was found, the minimum in the interaction curve was shifted to larger surface separation, and electrostatic repulsion was less apparent. Although the polymers used by Afshar-Rad et al. are not the same in the different experiments, these trends are in agreement with our calculations.

Marra and Hair[23] investigated the forces between two mica sheets covered with poly(2-vinylpyridine). The adsorption of the polyelectrolyte caused overcompensation of the surface charge. It was shown that, after initial repulsion due to double-layer overlap, bridge formation occurred. With an increasing amount of polyelectrolyte adsorbed, the minimum in the interaction was

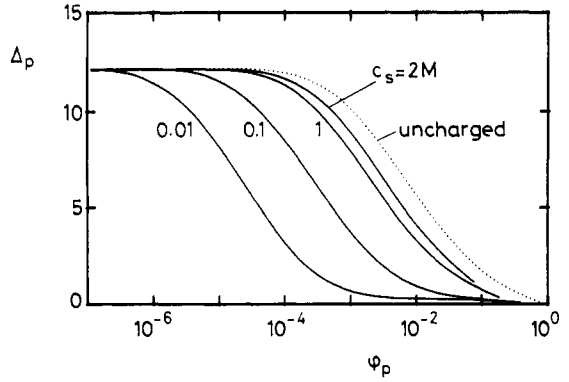

Figure 10. Depletion thickness as a function of the solution volume fraction of a fully charged polyelectrolyte, in four different salt concentrations (full curves) and for an uncharged polymer (dotted curve). The chain length is 500 segments; all χ parameters and the surface charge are zero.

less deep notwithstanding the stronger bridge formation. Upon neutralization of the polyelectrolyte, strong repulsive forces were measured due to steric and electrostatical effects. These trends corroborate our theoretical results.

Interaction by Depletion of Polyelectrolyte. Near a surface the conformational entropy of a polymer chain is decreased. This results in a repulsive force between surface and polymer, and, for nonadsorbing polymers, a depletion zone develops. The depletion thickness Δ_p, of polymer p, can be defined as

$$2\Delta_p = \frac{-\theta_p^{exc}}{\phi_p^{b}} \tag{26}$$

where θ_p^{exc}, the excess amount of nonadsorbing polymer p between the surfaces, is negative. In Figure 10 the depletion thickness of polyelectrolyte in four different salt concentrations is shown as a function of the solution volume fraction of polyelectrolyte. The polymer chains are 500 segments long and have a relative dielectric constant of 20. All Flory–Huggins interaction parameters are zero. The surfaces are uncharged. For comparison, the depletion thickness of an uncharged but otherwise identical polymer is plotted in the same figure (dotted curve). At very low solution volume fractions the depletion thicknesses of polyelectrolyte and uncharged polymer are equal. For polyelectrolyte in low salt concentration the decrease in depletion thickness with increasing polymer volume fraction sets in earlier than at high c_s. Thus, compared to uncharged polymer, more polyelectrolyte is present between the surfaces, especially at low ionic strength. If depletion of polyelectrolyte occurs, a potential must develop to maintain electroneutrality between the surfaces and an electrical double layer is formed. The electrostatic potentials in the double layer are attractive for the polyelectrolyte, and this explains the smaller depletion thickness of polyelectrolytes compared to uncharged polymers. The magnitude of the electrostatic potentials increases with the solution volume fraction of polyelectrolyte and decreases with salt concentration.

The free energy of interaction as a function of the separation between the surfaces is given in Figure 11. At very small surface separations, the polymer has left the gap between the surfaces and a Donnan equilibrium has been established. In this region two opposing effects occur. Because of the Donnan potential, the depletion thickness becomes smaller with decreasing ionic strength, whereas the osmotic pressure increases. This latter effect

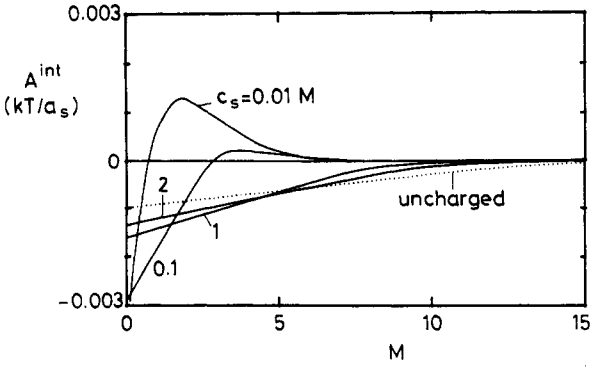

Figure 11. Free energy of interaction between two uncharged surfaces in the presence of polyelectrolyte, at different salt concentrations (full curve) and in the presence of uncharged polymer (dotted curve). The chain length is 500; the χ parameters are zero; the volume fraction in the bulk solution is 0.01.

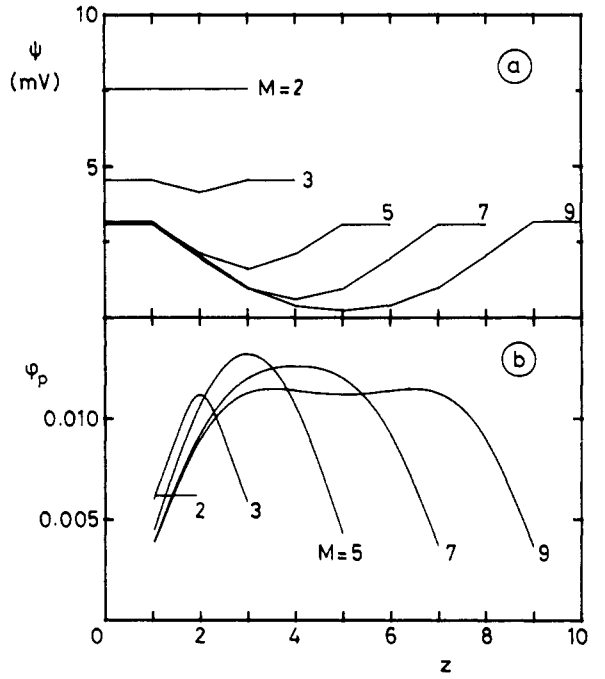

Figure 12. Potential profile (a) and the volume fraction profile of nonadsorbing polyelectrolyte (b) at different surface separations M (indicated). The salt concentration is 0.01 M, the chain length is 500 segments, all χ parameters and the surface charge are zero, and the volume fraction of polyelectrolyte in the solution is 0.01.

dominates at zero surface separation, so that there the free energy of interaction is lowest at zero salt concentration.

At low salt concentration, the interaction curve shows a maximum, caused by electrical double-layer repulsion. The double layer is shown in Figure 12a for c_s = 0.01 M and ϕ_p^{b} = 0.01. As the surfaces approach, the electrostatic potential in the middle of the gap increases. At small separations, the surface potential has increased as well, so that repulsion due to double-layer interaction can be expected. It is well-known[11] that repulsion decreases with increasing salt concentration, which explains that a repulsive part in the free energy of interaction is only present at low ionic strength.

The corresponding volume fraction profiles of polymer at different surface separations are given in Figure 12b. The volume fractions in the layers adjacent to the surface are much lower than the volume fractions in the middle of the gap. The interplay between electrostatic potentials and conformational restrictions leads to volume fractions in the middle of the gap that are higher

than those in the solution (in the case $\phi_p^b = 0.01$), except when M is large or smaller than 3.

Depletion interaction is much weaker than adsorption interaction. Consequently, the van der Waals attraction, which is not taken into account, may dominate the interaction curves. In spite of this complication, some evidence for the existence of depletion zones of polyelectrolyte near a nonadsorbing surface has recently been obtained by Marra and Hair.[24]

Conclusions

Electrostatic interactions and steric interactions can be successfully incorporated into a lattice theory. The multi-Stern-layer model as presented here offers a simple way to achieve this. With this model the adsorption of polyelectrolyte as a function of salt concentration and pH has been analyzed. If polyelectrolyte is fully charged, the adsorbed layer is thin. Increasing the salt concentration reduces the repulsion between segments, more chains adsorb, and the adsorbed layer becomes more extended. For weak polyacids a maximum in the adsorbed amount as a function of pH is found, 1–1.5 pH units below the pK. Due to the incorporation of the volume of salt ions in the theory, this maximum in the adsorbed amount is more pronounced than predicted by the model of Evers et al.,[5] which does not account for the volume of ions. The reason is that in the present model the adsorbed amount of uncharged polymer depends on the surface charge because of steric displacement of polymer segments by electrostatically adsorbing salt ions, whereas in the model of Evers et al. the surface charge has no effect on the adsorption of uncharged polymer.

At low adsorption energy, i.e., when adsorbed polyelectrolyte neutralizes the surface charge, the interaction between two surfaces is dominated by the amount of polymer between the surfaces. The interplay between attraction by polymer bridging and steric repulsion determines the net interaction. If, at high χ_{pS}, overcompensation of the surface charge occurs, electrostatic repulsion may control the interaction curves at large surface separations. If the polymer is uncharged, electrostatic repulsion between charged surfaces dominates the interaction curve and is felt at larger surface separation because the presence of polymer hinders the screening of the surface charge.

The depletion thickness of nonadsorbing polyelectrolyte decreases with decreasing salt concentration. When all polyelectrolyte has left the gap between the surfaces, a Donnan equilibrium has established. This leads to a stronger attraction between the surfaces than in the presence of uncharged polymers. However, in low salt concentrations a maximum in the interaction curve is found which may represent a strong repulsive barrier for two approaching surfaces.

Many properties of polyelectrolyte adsorption are similar to those of uncharged polymer in very good solvents. Examples are coil expansion in solution, high osmotic pressure, thin adsorption layers, low adsorbed amount, and thin depletion layers.

Appendix I

Numerical Method. The volume fraction profiles for all types of molecules can be calculated from eqs 3–10 if the potentials $u_i(z)$ are known. The potentials are given by eq 1 and depend on $u'(z)$ and the volume fractions, which in turn determine the charge densities and, consequently, the electrostatical potential profile. Hence, we have a set of simultaneous equations, and this set is to be solved numerically.

For each type of molecule i there are M unknown potentials $u_i(z)$ and M independent equations. The boundary conditions are that in every layer the sum of the volume fractions must be unity and that the system should not have a net charge.

Some molecules, e.g., molecules in restricted equilibrium and the molecules in layers 0 and $M + 1$, cannot adapt their amount between or on the surfaces to local conditions. The predetermined charge, σ_c, i.e., the net charge of these molecules, can be positive as well as negative. In order to neutralize σ_c, we need charged molecules of which we can rescale the amount during the iterations. We introduce a parameter t_i, which indicates the direction of rescaling and is 1 if molecules i are positive and −1 if molecules i are negative. For molecules that contribute to σ_c, we set $t_i = 0$. We set t_i also zero for the counterions of the weak polyacid, so that the degree of dissociation is not affected by rescaling the volume fractions. Obviously, for uncharged molecules t_i is also zero.

The relation between the iteration variables and the potentials is arbitrary. A convenient choice can be made if the iteration variable $x_i(z)$, its related to the potential, $u_i(z)$, in such a way that the segment weighting factor is insensitive to the average value of the iteration variables. Moreover, the iteration variable should contain information on the electrostatical potential with respect to the bulk solution and on the amount of polymer in the gap. The following relation fulfills these requirements:

$$x_i(z) = \frac{-u_i(z) + \bar{u}}{kT} + \left(\frac{t_i}{r_i} - \overline{\left(\frac{t}{r}\right)}\right)\frac{e\Delta\Psi}{kT} + \frac{\sum_i \ln G_i(r_i|1) + \sum_i \frac{t_i e\Delta\Psi}{kT}}{\sum_i \sum_z 1} \quad \text{(A1)}$$

The reference potential, $\Delta\Psi$, is the electrostatical potential difference between layer $M/2$ and the bulk solution. The average value of the potential $\bar{u}$ is defined as

$$\bar{u} = \frac{\sum_i \sum_z u_i(z)}{\sum_i \sum_z 1} \quad \text{(A2)}$$

and the average value of t_i/r_i as

$$\overline{\left(\frac{t}{r}\right)} = \frac{\sum_i (t_i/r_i)}{\sum_i 1} \quad \text{(A3)}$$

From eq A1 we obtain the sum of the iteration variables

$$\sum_i \sum_z x_i(z) = \sum_i \ln G_i(r_i|1) + \sum_i \frac{t_i e\Delta\Psi}{kT} \quad \text{(A4)}$$

and the deviation of the iteration variable from its average value

$$x_i(z) - \bar{x} = \frac{-u_i(z) + \bar{u} + \left(\frac{t_i}{r_i} - \overline{\left(\frac{t}{r}\right)}\right)e\Delta\Psi}{kT} \quad \text{(A5)}$$

where $\bar{x}$ is the average value of all iteration variables. We define a reduced segment weighting factor, $\tilde{G}_i(z)$, which

can be obtained from the iteration variables directly

$$\tilde{G}_i(z) = \exp(x_i(z) - \tilde{x}) \tag{A6}$$

By substitution of eq A5 into eq A6, we obtain with eq 3

$$\tilde{G}_i(z) = G_i(z) \exp\left(\frac{\bar{u} + \left(\frac{t_i}{r_i} - \overline{\left(\frac{t}{r}\right)}\right)e\Delta\Psi}{kT}\right) \tag{A7}$$

The exponent contains two terms that are independent of i and a term that depends on the value of t_i. From the reduced segment weighting factors, reduced end-segment distribution functions can be calculated using an equivalent of eq 5:

$$\tilde{G}_i(z,s|1) = \tilde{G}_i(z)(\lambda_1\tilde{G}_i(z-1,s-1|1) + \lambda_0\tilde{G}_i(z,s-1|1) + \lambda\tilde{G}_i(z+1,s-1|1)) \tag{A8}$$

The reduced chain weighting factors are calculated from an equivalent of eq 6:

$$\tilde{G}_i(r_i|1) = \sum_z \tilde{G}_i(z,r_i|1) \tag{A9}$$

The relation between the reduced chain weighting factor and the chain weighting factor is given by

$$\tilde{G}_i(r_i|1) = G_i(r_i|1) \exp\left(\frac{t_i e\Delta\Psi}{kT} + \frac{r_i}{kT}\left(\bar{u} - \overline{\left(\frac{t}{r}\right)}e\Delta\Psi\right)\right) \tag{A10}$$

so that in combination with eq A4 the second term in the exponent can be calculated:

$$\frac{\bar{u} - \overline{\left(\frac{t}{r}\right)}e\Delta\Psi}{kT} = \frac{\sum_i \ln \tilde{G}_i(r_i|1) - \sum_i\sum_z x_i(z)}{\sum_i r_i} \tag{A11}$$

The reduced amount of molecule i is defined as:

$$\tilde{\theta}_i = \theta_i \exp\left(\frac{t_i e\Delta\Psi}{kT}\right) \tag{A12}$$

From the combination of eqs 10a, 10b, A12, and A10, the reduced amount of molecule i can now be obtained from:

$$\ln \tilde{\theta}_i = \ln \phi_i^{\,b} + \ln \tilde{G}_i(r_i|1) - \frac{r_i}{kT}\left(\bar{u} - \overline{\left(\frac{t}{r}\right)}e\Delta\Psi\right) \tag{A13}$$

The reduced normalization constant is calculated with the equivalent of eq 10a:

$$\tilde{C}_i = \frac{\tilde{\theta}_i}{r_i\tilde{G}_i(r_i|1)} \tag{A14}$$

Reduced volume fractions $\tilde{\phi}_i$ are calculated from the reduced end-segment distribution functions with the equivalent of eq 7:

$$\tilde{\phi}_i(z,s) = \frac{\tilde{C}_i\tilde{G}_i(z,s|1)\,\tilde{G}_i(z,s|r)}{\tilde{G}_i(z)} \tag{A15}$$

If $t_i = 0$, the volume fractions are equal to the reduced volume fractions because the second term in the exponent of eq A10 cancels in eq A15. Analogous to eq A12, the relation between the volume fraction and the reduced volume fraction is given by:

$$\phi_i(z,s) = \tilde{\phi}_i(z,s) \exp\left(\frac{-t_i e\Delta\Psi}{kT}\right) \tag{A16}$$

The value of $\Delta\Psi$ follows from the electroneutrality condition, which can be formulated as:

$$\sum_+ \frac{v_i e\bar{\alpha}_i\theta_i}{a_s} + \sum_- \frac{v_i e\bar{\alpha}_i\theta_i}{a_s} + \sigma_c = 0 \tag{A17}$$

The first summation extends only over the molecules with $t_i = 1$, and the second summation, over the molecules with $t_i = -1$. The weighted average of the degree of dissociation is

$$\bar{\alpha}_i = \frac{\sum_z \alpha_i(z)\,\tilde{\phi}_i(z)}{\sum_z \tilde{\phi}_i(z)} \tag{A18}$$

Substitution of eq A12 into eq A17 leads to:

$$\sum_+ \frac{v_i e\bar{\alpha}_i\tilde{\theta}_i \exp\left(\frac{-e\Delta\Psi}{kT}\right)}{a_s} + \sum_- \frac{v_i e\bar{\alpha}_i\tilde{\theta}_i \exp\left(\frac{e\Delta\Psi}{kT}\right)}{a_s} + \sigma_c = 0 \tag{A19}$$

Equation A19 is transformed into a quadratic equation from which $e\Delta\Psi/kT$ can be solved as:

$$\exp\left(\frac{e\Delta\Psi}{kT}\right) = \frac{-\sigma_c - \left[(\sigma_c)^2 - 4\sum_+ \frac{v_i e\bar{\alpha}_i\tilde{\theta}_i}{a_s}\sum_- \frac{v_i e\bar{\alpha}_i\tilde{\theta}_i}{a_s}\right]^{1/2}}{2\sum_- \frac{v_i e\bar{\alpha}_i\tilde{\theta}_i}{a_s}} \tag{A20}$$

With eq A16 the volume fractions can now be calculated from the reduced volume fractions, and with eqs A7 and A11 the segment weighting factors are calculated from the reduced weighting factors. Starting from $\Delta\Psi$ in layer $M/2$ the electrostatical potentials are calculated with eq 17. The hard-core potential of molecules i in layer z is calculated from eq 1:

$$u_i'(z) = u_i(z) - kT\sum_j \chi_{ij}\left\{\frac{\langle\phi_j(z)\rangle}{\sum_j \phi_j(z)} - \phi_j^{\,b}\right\} - v_i\alpha_i(z)e\Psi_i(z) \tag{A21}$$

We calculate the average $u'(z)$:

$$u'(z) = \frac{1}{\sum_i 1}\sum_i u_i'(z) \tag{A22}$$

A function is defined that is only zero if the sum of the volume fractions are unity in each layer and if the local hard-core potential is the same for every segment in the same layer:

$$f_i(z) = 1 - \frac{1}{\sum_i \phi_i(z)} - u_i'(z) + u'(z) \tag{A23}$$

The point of zero of this function of the iteration variables $x_i(z)$ can be found numerically by standard methods.

In the numerical calculations we may save computing time by exploiting the symmetry of the system. We place a reflecting boundary in the middle of the system, thereby reducing the number of equations to $M/2$ per molecule type. We also make use of the symmetry of the chain molecules, similar to ref 6.

In the calculations on weak polyacids the number of different molecules is 6: H_2O, OH^-, H_3O^+, positive salt ions, negative salt ions, and polyacid. In these calculations the number of molecules is reduced to 5 by treating water as a weak electrolyte with valency −1. The dissociation equilibrium of water is incorporated as $pK_w = 14 - 2 \log (10^3 N_A a_s d) = 15.4$ (eq 24 for $\phi_w = 1$; here N_A is Avogadro's number and $d = 0.6$ nm). The degree of dissociation of water in every layer z is calculated with eq 13.

Appendix II

List of Symbols

$A(M)$	free energy of a system between two surfaces at separation M
$A^\sigma(M)$	Gibbs excess free energy of a system between two surfaces at separation M
C_i	normalization constant for molecules i
D	distance from the solid/liquid boundary
$D(z)$	electric displacement in layer z
$E(z)$	field strength in layer z
$G_i(z)$	segment weighting factor for segments i in layer z
$G_i(z,s\|1)$	end-segment distribution function in layer z of molecules i (s segments long), with segment 1 in an arbitrary layer
$G_i(z,s\|r)$	end-segment distribution function in layer z of molecules i ($r - s + 1$ segments long), with segment r in an arbitrary layer
$G_i(r\|1)$	chain weighting factor of molecules i
K_i	dissociation constant for segments i, expressed as a dimensionless quantity
K_d	dissociation constant in moles per cubic decimeter
L	number of lattice sites per lattice layer
M	number of lattice layers between the surfaces
N_A	Avogadro's number
S	subscript indicating the solid
T	absolute temperature
U_{el}	electrical energy
Z	number of neighboring lattice sites
a_s	cross-sectional area of a lattice site
c_i, c_s	concentration of molecules i, salt concentration
d	distance between two lattice layers
e	elementary charge
i,j	index for molecule or segment type
k	Boltzmann's constant
p	subscript used to indicate polymers
r_i	chain length of molecule i
s	segment ranking number
$u_i(z)$	potential for segments of type i in layer z
$u'(z)$	hard-core potential in layer z
v_i	valency of segment i
z	layer number
$\alpha_i(z)$	degree of dissociation of segments of molecules i in layer z
α_i^b	degree of dissociation of segments of molecules i in bulk solution
Δ_i	depletion thickness of molecules i
ϵ_0	dielectric permittivity in vacuo
ϵ_i	dielectric permittivity of molecules i
$\epsilon(z)$	dielectric permittivity in layer z
θ_i	amount of molecules i (in equivalent monolayers) between the surfaces
θ_i^a	adsorbed amount of molecules i (on one surface)
θ_i^{exc}	excess amount of molecule i between the surfaces with respect to the homogeneous bulk solution
λ_0	fraction of neighboring lattice sites in the same layer
λ_1	fraction of neighboring lattice sites in the adjacent layer
μ_i	chemical potential of molecules i
$\phi_i(z)$	volume fraction of segments i in layer z
$\langle\phi_i(z)\rangle$	fraction of contacts of a site in layer z with segments i
ϕ_i^b	volume fraction of molecule i in the bulk solution
$\phi_i^f(z)$	volume fraction of nonadsorbed molecules i in layer z
$\phi_i(z,s)$	volume fraction of segment s of molecule i in layer z
$\Psi(z)$	electrostatic potential in layer z
χ_{ij}	Flory–Huggins interaction parameter between i and j
$\sigma(z)$	charge on the plane in the center of layer z

Additional Symbols in Appendix I

$\tilde{C}_i$	reduced normalization constant of molecule i
$\tilde{G}_i(z)$	reduced segment weighting factor
$\tilde{G}_i(z,s\|1)$	reduced end-segment distribution function in layer z of molecules i (s segments long) with segment 1 in an arbitrary layer
$\tilde{G}_i(z,s\|r)$	reduced end-segment distribution function of molecules i ($r - s + 1$ segments long) in layer z with segment r in an arbitrary layer
$\tilde{G}_i(r\|1)$	reduced chain weighting factor of molecule i between the surfaces
t_i	direction of rescaling for molecule i
$u_i'(z)$	apparent hard-core potential for segment i in layer z during the iterations
$\bar{u}$	average value of all potentials
w	subscript indicating the solvent (water)
$x_i(z)$	iteration variable for segment i in layer z
$\bar{x}$	average value of all iteration variables
$\bar{\alpha}_i$	weighted average of the degree of dissociation of segment i
$\tilde{\theta}_i$	reduced amount of molecule i
$\tilde{\phi}_i(z,s)$	reduced volume fraction of segment s of molecule i in layer z
$\Delta\Psi$	electrostatic reference potential
σ_c	fixed charge, i.e., the contribution of molecules with $t_i = 0$ to the total charge

References and Notes

(1) Van der Schee, H. A.; Lyklema, J. *J. Phys. Chem.* **1984**, *88*, 6661.
(2) Roe, R. J. *J. Chem. Phys.* **1974**, *60*, 4192.
(3) Scheutjens, J. M. H. M.; Fleer, G. J. *J. Phys. Chem.* **1979**, *83*, 1619.
(4) Scheutjens, J. M. H. M.; Fleer, G. J. *J. Phys. Chem.* **1980**, *84*, 178.
(5) Evers, O. A.; Fleer, G. J.; Scheutjens, J. M. H. M.; Lyklema, J. *J. Colloid Interface Sci.* **1986**, *111*, 446.
(6) Scheutjens, J. M. H. M.; Fleer, G. J. *Macromolecules* **1985**, *18*, 1882.
(7) Fleer, G. J.; Scheutjens, J. M. H. M. *J. Colloid Interface Sci.* **1986**, *111*, 504.
(8) Lyklema, J.; Fleer, G. J. *Colloids Surf.* **1987**, *25*, 357.
(9) Muthukumar, M. *J. Phys. Chem.* **1987**, *86*, 7230.
(10) Evers, O. A. Ph.D. Thesis, Wageningen Agricultural University, The Netherlands, 1990.
(11) Verwey, E. J. W.; Overbeek, Th. O. *Theory on the Stability of Lyophobic Colloids*; Elsevier: Amsterdam, The Netherlands, 1948.
(12) Carney, S. L.; Torrie, G. M. *Adv. Chem. Phys.* **1984**, *56*, 141.
(13) Marra, J.; Van der Schee, H. A.; Fleer, G. J.; Lyklema, J. In *Adsorption from Solution*; Ottewill, R. H., Rochester, C. H., Smith, A. L., Eds.; Academic Press: London, 1983, p 245.

(14) Bonekamp, B. C.; Van der Schee, H. A.; Lyklema, J. *Croat. Chem. Acta* **1983**, *56*, 695.
(15) Papenhuyzen, J.; Fleer, G. J.; Bijsterbosch, B. H. *J. Colloid Interface Sci.* **1985**, *104*, 530.
(16) Cosgrove, T.; Obey, T. M.; Vincent, B. *J. Colloid Interface Sci.* **1986**, *111*, 409.
(17) Blaakmeer, J.; Böhmer, M. R.; Cohen Stuart, M. A.; Fleer, G. J. *Macromolecules*, succeeding paper in this issue.
(18) Cafe, M. C.; Robb, I. D. *J. Colloid Interface Sci.* **1982**, *86*, 411.
(19) Robb, I. D.; Sharples, M. *J. Colloid Interface Sci.* **1982**, *89*, 301.
(20) Foissy, A.; El Attar, A.; Lamarche, J. M. *J. Colloid Interface Sci.* **1983**, *96*, 275.
(21) Durand-Piana, G.; Lafuma, F.; Audebert, R. *J. Colloid Interface Sci.* **1987**, *119*, 474.
(22) Afshar-Rad, T.; Bailey, A. I.; Luckham, P. F.; MacNaughtan, W.; Chapman, D. *Colloids Surf.* **1988**, *31*, 125.
(23) Marra, J.; Hair, M. L. *J. Phys. Chem.* **1988**, *92*, 6044.
(24) Marra, J.; Hair, M. L. *J. Colloid Interface Sci.* **1989**, *128*, 511.

Adsorption of Weak Polyelectrolytes on Highly Charged Surfaces. Poly(acrylic acid) on Polystyrene Latex with Strong Cationic Groups

J. Blaakmeer, M. R. Böhmer, M. A. Cohen Stuart, and G. J. Fleer*

Laboratory for Physical and Colloid Chemistry, Wageningen Agricultural University, Dreijenplein 6, 6703 HB Wageningen, The Netherlands. *Received June 26, 1989; Revised Manuscript Received October 18, 1989*

ABSTRACT: We have studied the adsorption of the weak polyelectrolyte poly(acrylic acid) (PAA) on a positively charged polystyrene latex. The latex surface contained quaternary ammonium groups, so that the surface charge was independent of pH. Hence, when the pH was changed, only the degree of dissociation of the polymer varied. We found that the adsorbed amount is low at high pH, where PAA is fully charged. With decreasing pH the adsorption increases and passes through a maximum at about 1 pH unit below the intrinsic dissociation constant pK_0 of the carboxylic groups of the macromolecule. The ionic strength has little effect. The experimental results agree very well with a recent extension[1] of the model of Scheutjens and Fleer to polyelectrolyte adsorption.

Introduction

The adsorption of polymeric materials plays an important role in a number of technological processes such as waste water treatment, flotation separations, fine-particle recovery by selective flocculation, enhanced oil recovery, etc.[2-5] Much effort has been put into experimental and theoretical work to understand the behavior of polymers at interfaces. Gradually, the main trends in the adsorption behavior of neutral polymers and polyelectrolytes on charged and uncharged surfaces become clear.

For the adsorption of neutral polymers one generally finds thick adsorbed layers and long tails with many segments of the adsorbed polymer in loops. In good solvents the adsorbed amount is low and only weakly dependent on chain length. However, in poor solvents (Θ solvents) the adsorbed amount depends linearly on the logarithm of the molecular weight of the polymer. When the ionic strength is increased, the adsorption of a neutral polymer may increase because the solvent quality decreases with increasing salt concentration.[6,7] Charging the surface has only a minor effect on the interfacial behavior of uncharged macromolecules. However, the adsorbed amount on a charged surface is less than on an uncharged surface if the number of available sites for binding the polymer decreases on charging the surface. This is the case for the adsorption of poly(vinyl pyrrolidone) and poly(ethylene oxide) onto silica.[8] Those polymers adsorb by hydrogen bonding with SiOH groups, the number of which decreases with increasing pH. Another effect of the surface charge on the adsorption of uncharged polymers has recently been predicted theoretically.[1] If the surface charge is very high, the accumulation of counterions in the double layer prevents high polymer segment concentrations and decreases the adsorbed amount. As far as we are aware, no experimental study has, as yet, dealt with this effect.

For polyelectrolyte adsorption, we have to make a distinction between strong and weak polyelectrolytes. Some general trends in the adsorption of strong polyelectrolytes, for which the charge does not depend on pH, have been discussed by Cohen Stuart.[9] For media with relatively low ionic strength ($c_s < 0.2$ M) and a neutral surface, the charged polyelectrolyte will adsorb in a flat configuration. In this case the adsorbed amount is low, and there is no dependence on molecular weight or ionic strength. For media with a relatively high ionic strength ($c_s > 1$ M), the adsorption is a function of the ionic strength and the molecular weight. The trends of the adsorption are, in this ionic strength region, comparable to the adsorption of a neutral polymer. When the surface is oppositely charged, the adsorbed amount of a strong polyelectrolyte depends on the surface charge density, resulting in higher adsorbed amounts for surfaces with higher surface charge densities because of the electrostatic contribution to the adsorption energy of the segments.

For weak polyelectrolytes, the degree of dissociation, α, depends on the pH. At low pH, where $\alpha = 0$ (polyacid), the situation is similar to that for the adsorption of neutral polymers. In the limit of high pH, where $\alpha =$

* To whom all correspondence should be addressed.

0024-9297/90/2223-2301$02.50/0